UAV-assisted Multiple Access Computation Offloading and Resource Allocation in Ocean Monitoring Network

Yuxuan Ji[1,2], *Qi Zhu*[1,2*]

[1] *Jiangsu Key Laboratory of Wireless Communications, Nanjing University of Posts and Telecommunications, China*
[2] *Engineering Research Center of Health Service System Based on Ubiquitous Wireless Networks, Nanjing University of Posts and Telecommunications, China*
jyx001012@163.com, zhuqi@njupt.edu.cn

Abstract

Given the swift evolution of oceanic surveillance systems and the substantial expansion of diverse marine intelligent devices and services, the serious attenuation of the acoustic channels in underwater sensor networks and the scarce computing resources of the ocean surface have led to the inability to meet the requirements of Unmanned Surface vehicle (USV) users for low latency and low energy consumption. This paper constructs an unmanned aerial vehicle (UAV)-assisted multi-access computing offloading model in ocean monitoring networks. Specifically, in the data collection stage, Underwater sensor nodes (USNs) transmit the collected data to the USVs via non-orthogonal multiple access (NOMA). In the data processing stage, USVs offloads part of the data to the UAV via frequency division multiple access (FDMA), and the UAV and USVs cooperate to complete the data processing task. In order to meet the requirements of USVs, this paper introduces a joint optimization problem, which involves optimizing the USN's transmission power, USV's transmission power, USV's offloading decision, and USV's bandwidth allocation. Considering the independence between the two stages, the optimization problem is decomposed into two separate stage-problems. The optimization problem of the data collection stage enables collected data to arrive at the USV simultaneously by using the particle swarm optimization algorithm to control the USN's transmission power. The optimization problem of the data processing stage is decomposed into three sub-problems: the USV's transmission power, USV's offloading decision, and USV's bandwidth allocation, which are optimized separately by using gradient descent, genetic algorithm, and CVX solver respectively. Through iterative alternation, the optimal solution of the data processing stage can be obtained. The simulation results demonstrate a considerable decrease in sum of latency and energy consumption for USVs with the proposed algorithm.

Keywords: Mobile Edge Computing (MEC), Ocean Monitoring Networks (OMNs), Unmanned Aerial Vehicle (UAV), Computational offloading, Resource allocation

1 Introduction

As an essential component of the intelligent ocean information network, Ocean Monitoring Networks (OMNs) connect various types of vessels, underwater sensors, drones, and satellites. They serve as crucial platforms for collecting various resource data such as ocean environment, resources, and space. By deploying underwater sensor nodes (USNs), OMNs gather seabed information sensed by sensors and transmit it to surface-demanding users. New computationally intensive maritime applications, including marine resource exploration, vessel navigation assistance, and marine disaster prevention can greatly benefit from the ubiquitous Internet services offered by ocean monitoring networks. With the significant growth of various marine intelligent devices and businesses [1-2], ensuring the positive experience of surface users has becoming an enormous challenge [3]. By introducing Mobile Edge Computing (MEC) technology into ocean monitoring sensor networks, data centers can be deployed to the network edge, providing nearby data processing and storage services.

Research on underwater sensor networks has yielded many results. Underwater acoustic transmission encounters drawbacks like restricted bandwidth, low data transmission rates, and substantial environmental noise [4], its favorable stability, affordability, and simplicity remain key factors driving its adoption in practical scenarios. Moreover, USNs, powered by batteries and positioned on the seabed for data sensing, face the challenge of energy consumption due to acoustic signal attenuation. Given their impracticality for frequent battery replacement, these optimizations extend the lifespan of USNs [5-6]. In [7], Liu et al. studied the problem of extending the lifecycle of underwater sensor networks. It proposed a joint optimization problem regarding relay node deployment and traffic allocation and reduced energy consumption through a heuristic scheme based on a three-dimensional structure. To further extend the network lifecycle, [8] iteratively updates each node's relay selection and data flow by using a heuristic routing scheme.

With the continuous growth of demand for marine intelligent services, scarce marine computing resources cannot meet the high requirements of sea-surface users for low latency and low energy consumption. Therefore,

*Corresponding Author: Qi Zhu; Email: zhuqi@njupt.edu.cn
DOI: https://doi.org/10.70003/160792642026072704004

how to flexibly adapt the computation offloading strategy of ocean monitoring sensor networks is a primary issue to be addressed and has received significant attention from researchers in recent years. [9] introduced a method to approximate the sea-surface channel, addressing the upper limit of throughput concerning its complexity. By optimizing both communication resource allocation and trajectory simultaneously, the minimum expected throughput of all vessels was maximized. In [10], Yang et al. constructed an integrated communication network for sea, air, and space. They introduced a two-stage optimal algorithm tailored to diverse quality of service (QoS) requirements in intricate marine settings. This algorithm optimized the distribution of computation and communication resources while considering constraints on energy and sensitivity to delays. In [11], Yang et al. investigated the problem of ship selection of appropriate Mobile Edge Computing service nodes for computation offloading in scenarios with multiple ships and multiple MEC service nodes at sea, and proposed an improved Hungarian multiple-ship computation offloading algorithm. [12] suggested a model consisting of combined offloading across multiple edges. By using an optimization method based on improved antlered search, marine mobile devices quickly obtain offloading strategies to maximize task execution efficiency. The edge servers mentioned in the above papers are all deployed in coastal edge networks, but ground-based stations are difficult to construct in offshore scenarios.

In recent years, the scenario of applying Unmanned Aerial Vehicles (UAVs) to maritime networks and assisting surface users in computation offloading has begun to attract increasing attention. As a type of mobile computing server, UAVs can be rapidly deployed and flexibly offloaded in maritime communication networks. Additionally, because UAVs usually hover at high altitudes, the channel model between UAVs and surface users can be reasonably established as a line-of-sight (Los) transmission link, potentially increasing the data transmission rate. In [13], Li et al. introduced UAV into maritime communication to compensate for the long delay of satellite communication, forming a hybrid model of satellite-UAV-ground, and enhanced the coverage of the maritime network by deploying UAVs. In [14], Liu et al. constructed a two-layer UAV model consisting of an upper-level UAV and distributed lower-level UAVs. UAV swarms provided efficient computing capabilities through resource sharing and shortened task completion delays under limited resources. Ma et al. [15] proposed a UAV-assisted maritime monitoring network model for data collection. It aimed to maximize network lifespan and models the multiple access, resource allocation, and UAV deployment problems as a mixed-integer non-convex optimization problem. Dai et al. [16] investigated UAV-assisted multiple access computation offloading in maritime networks. It aimed to minimize the total energy consumption of USNs and surface UAVs and jointly optimizes the upload time of USNs, computation offloading decisions of UAVs, offloading time, and confidentiality configuration.

Most existing studies about task offloading in OMNs only focus on the data processing stage, neglecting the underwater data collection stage [9-14]. However, due to the low transmission rate and limited bandwidth of acoustic signals underwater, the data collection stage often incurs significant latency, making end-to-end timely transmission a challenge that cannot be ignored. To simultaneously consider the underwater data collection stage and the data processing stage, USVs are deployed on the ocean surface to receive and process the data sent by USNs. USVs have higher speed and lower endurance, making them more susceptible to the influence of the ocean environment. Dai et al. [16] deployed USVs in OMNS, and aimed to minimize the total energy consumption of USNs and UAVs. However, overcoming the impact of the ocean environment on the hull increases the energy consumption of USVs, while their remote offshore location makes charging very difficult, which means that reducing the energy consumption of USVs is crucial. In addition, once USNs detect abnormal marine signals such as earthquakes or tsunamis, these signals must be immediately processed by USVs. Therefore, it is necessary to discuss both the latency and energy consumption of USVs. Motivated by these considerations, we investigate a UAV-assisted computation offloading model via hybrid NOMA and FDMA in OMNs, considering both the data collection and data processing stages. With the objective of minimizing the weighted sum of latency and energy consumption for USVs, we propose a jointly optimization problem. The main innovative points of this paper as follows:

(1) Constructed a UAV-assisted maritime monitoring network multiple access computation offloading model, which consists of two stages. In the data collection stage, the USNs transmit collected data to USVs via Non-Orthogonal Multiple Access (NOMA). In the data processing stage, the UAV act as an airborne server hovering in the air, while USVs offload part of the data to the UAV via frequency division multiple access (FDMA). The UAV and USVs collaborate to complete data processing tasks. The joint optimization problem of the whole task completion process was established with the objective of minimizing the weighted sum of latency and energy consumption for surface users. The joint optimization problem was decoupled into two separate stage-problems, and then solved sequentially.

(2) In the data collection stage, USNs utilize NOMA to upload data to improve channel utilization. Since users process data only after collecting all sensors' data, minimizing data collection latency is equivalent to minimizing the maximum latency of underwater sensors. In situations where communication resources are limited, minimizing data collection latency requires all sensor data to arrive at the USV simultaneously. In this paper, we enable collected data to arrive at the USV simultaneously by using the particle swarm optimization algorithm to control the USN's transmission power.

(3) In the data processing stage, USVs offload part of the tasks to the UAV via FDMA, and the tasks are jointly completed by USVs and the UAV. Since the optimization problem in the data processing stage is still non-convex, it is further decomposed into three sub-problems:

optimization of the USV's transmit power, offloading decision, and bandwidth allocation. These sub-problems are solved respectively by using gradient descent method, genetic algorithm, and CVX solver.

The subsequent sections of this paper are structured as follows: Section 2 presents the system model for data collection and computation offloading of USVs in UAV-assisted maritime monitoring network scenarios. It constructs the optimization problem of minimizing the weighed sum of latency and energy consumption for USVs. Section 3 decomposes the optimization problem into optimization sub-problems of two stages and solves the optimization sub-problems of the two stages using different algorithms. Section 4 conducts simulation and analysis of the algorithms. Section 5 provides a summary. To facilitate reading, commonly used symbols and their meanings are added in Table 1. The contents of Table 1 are as follows:

Table 1. Symbols used in paper

Symbols	Meanings
$P_{k,i}$	$USN_{k,i}$'s transmit power
$r_{k,i}$	$USN_{k,i}$'s transmission rate
$g_{k,i}$	channel gain between $USN_{k,i}$ and USV_k
r_k	data rate between USV_k and UAV
p_k	USV_k's transmit power
$R_{k,i}$	the amount of data collected by $USN_{k,i}$
B_k	USV_k's bandwidth
R_k	the amount of data of USV_k
t_k^{local}	USV_k's local processing latency
t_k^{off}	USV_k's offloading latency
t_k^{proc}	USV_k's task processing latency
E_k^{local}	USV_k's computational energy consumption
E_k^{trans}	USV_k's transmission energy consumption
E_k	USV_k's total energy consumption

2 Problem Formulation

2.1 System Model

Figure 1 illustrates the UAV-assisted multiple access computation offloading model proposed in this paper, which constitutes a maritime monitoring network composed of multiple USNs, multiple USVs, and a single UAV. The UAV hovers at a fixed altitude above USVs. In the underwater data collection stage, data collected by USNs is transmitted to USVs through underwater acoustic channels, employing NOMA to enhance channel utilization. In the surface data processing stage, the UAV serves as a mobile edge station assisting USVs in processing data, while USVs themselves possess a certain level of computing capability. In the data processing stage, USVs locally process a portion of the data and offload the remaining data to the UAV for processing via Frequency Division Multiple Access (FDMA).

There are K USV users deployed on the sea surface and M USNs deployed on the seabed. The set of USVs is denoted as $\mathcal{K} = \{1, ..., k, ..., K\}$. The set of USNs is denoted as $\mathcal{M} = \{1, ..., m, ..., M\}$. USNs are divided into K clusters as $\mathcal{M}_1, ..., \mathcal{M}_k, ..., \mathcal{M}_K$, with each cluster of USNs corresponding to one USV user. USNs detect marine environments and transmit the detected data to USV users. After receiving all the data sent by USNs, each USV user needs to immediately process the collected data. Let the data processing task for the kth USV user be denoted as $\left(C_k, R_k, \kappa, T_k^{\max}, E_k^{\max}\right)$, where C_k represents the total CPU required for the task, R_k represents the total number of bits for the task, κ represents the task complexity, and $C_k = \kappa R_k$. $T_k^{\max}$ represents the tolerable latency for completing the task, and $E_k^{\max}$ represents the upper limit of energy consumption for completing the task. β_k represents the offloading ratio of the kth user, where the amount of data processed locally by the kth user is $(1-\beta_k)R_k$, and the amount of data offloaded is $\beta_k R_k$.

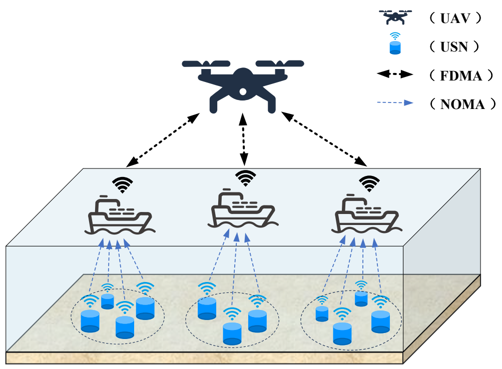

Figure 1. System model

Figure 2 illustrates the flow of data collection and processing in the system model proposed in this paper. Assuming the channel information of USVs and USNs is known. The specific process for the flow is as follows:

① The UAV sends data collection commands to USVs;

② USVs receive the data collection commands and execute Algorithm 1 to obtain the optimal transmission power scheme for USNs;

③ USVs send data collection commands and information about the optimal transmission power scheme to USNs;

④ USNs send the collected data to USVs using the optimal transmission power;

⑤ USVs send information about the amount of collected data to the UAV;

⑥ The UAV executes a joint optimization algorithm of the USV's transmission power, bandwidth, and offloading ratio to obtain the optimal USV's transmission power scheme, bandwidth allocation and offloading decision;

⑦ The UAV sends the information about USV's optimal transmission power scheme, bandwidth allocation and offloading decision to USVs;

⑧ USVs process part of the data locally and send the rest to the UAV using the optimal transmission power and bandwidth.

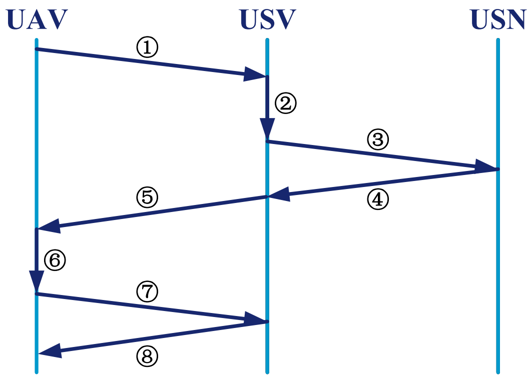

Figure 2. Flow of data collection and processing

2.2 Communication Model

The whole data completion process in this paper has two stages. In the underwater data collection stage, USNs first transmit the collected data to USVs via NOMA. In the data processing stage, USVs offloads part of the data to the UAV via FDMA, and the UAV and USVs jointly accomplish the computation task. Due to the different communication environments in the data collection stage (underwater communication) and the data processing stage (on-water communication), it is necessary to discuss them separately.

2.2.1 The Data Collection Stage

Each USV has a limited coverage range, within which several USNs are distributed. Without loss of generality, analyze the USNs within the coverage range of USV_k. Assume there are I USNs within the coverage range of USV_k, denote these USNs as $USN_{k,i}$ and denote the set of these USNs as $\mathcal{I} = \{1, ..., i, ... I\}$.

Represent $USN_{k,i}$'s position as $(x_{k,i}, y_{k,i}, z_{k,i})$, and represent USV_k's position as $(x_k, y_k, 0)$. The distance between $USN_{k,i}$ and USV_k can be calculated as:

$$d_{k,i} = \sqrt{(x_{k,i} - x_k)^2 + (y_{k,i} - y_k)^2 + z_{k,i}^2} \tag{1}$$

$USN_{k,i}$ transmit date to USV_k through the underwater acoustic channel, and the model for the channel can be represented as [4]:

$$\mathcal{F}\left(d_{k,i}, \theta\right) = d_{k,i}^{\gamma} \mathcal{L}\left(\theta\right)^{\frac{d_{k,i}}{1000}}, \quad \forall i \in \mathcal{I} \tag{2}$$

where $\mathcal{F}(d_{k,i}, \theta)$ represents the attenuation of the acoustic signal, parameter γ is the spreading factor, parameter θ is the center frequency of the acoustic signal, and $\mathcal{L}(\theta)$ is the absorption coefficient.

The absorption coefficient $\mathcal{L}(\theta)$ is obtained according to Thorp's empirical formula [4]:

$$\mathcal{L}\left(\theta\right) = \frac{0.11\theta^2}{1+\theta^2} + \frac{44\theta^2}{4100+\theta^2} + 2.75\times 10^{-4}\theta^2 + 0.003 \tag{3}$$

Unlike traditional white noise, acoustic signals are commonly influenced by ocean noise during transmission. Ocean noise typically consists of four main components: turbulence, vessel-generated noise, wind and wave disturbances, and thermal noise, represented as [15]:

$$10\log_{10} W_1\left(\theta\right) = 17 - 30\log_{10}\theta \tag{4}$$

$$\begin{aligned} 10\log_{10} W_2\left(\theta\right) &= 40 + 20\left(a - 0.5\right) \\ &+ 26\log_{10}\theta - 60\log_{10}\left(\theta + 0.03\right) \end{aligned} \tag{5}$$

$$\begin{aligned} 10\log_{10} W_3\left(\theta\right) &= 50 + 7.5b^{0.5} \\ &+ 20\log_{10}\theta - 40\log_{10}\left(\theta + 0.4\right) \end{aligned} \tag{6}$$

$$10\log_{10} W_4\left(\theta\right) = -15 + 20\log_{10}\theta \tag{7}$$

where a represents the coefficient of vessel activity and b represents wind speed, measured in meters per second.

The noise power density $W(\theta)$ is expressed as:

$$W\left(\theta\right) = W_1\left(\theta\right) + W_2\left(\theta\right) + W_3\left(\theta\right) + W_4\left(\theta\right) \tag{8}$$

The channel gain between $USN_{k,i}$ and USV_k can be calculated as [15]:

$$g_{k,i} = \frac{1}{\mathcal{F}\left(d_{k,i}, \theta\right) W(\theta) B_{usn}}, i \in \mathcal{I} \tag{9}$$

Due to the utilization of NOMA technology, USNs within the coverage area of the same USV share the same channel. Therefore, there will be mutual interference among USNs within the coverage area of the same USV. Arrange USN's transmitted signals in descending order of received power:

$$P_{k,1}g_{k,1} > P_{k,2}g_{k,2} > \cdots > P_{k,i}g_{k,i} > \cdots > P_{k,I}g_{k,I} \tag{10}$$

When $USN_{k,i}$ sends data to USV_k, the transmission rate $r_{i,k}$ for $USN_{k,i}$ uploading data to USV_k can be represented as:

$$r_{k,i} = B_{usn}\log_2\left(1 + \frac{P_{k,i}g_{k,i}}{\sum_{\substack{j\in\mathcal{I} \\ j>i}} P_{k,j}g_{k,j} + \sigma^2}\right), \forall i \in \mathcal{I} \tag{11}$$

where B_{usn} is the USN's channel bandwidth, $P_{k,i}$ is the $USN_{k,i}$'s transmit power, σ^2 represents the white Gaussian noise power at USNs.

2.2.2 The Data Processing Stage

The UAV hovers at a fixed altitude and acts as an edge server to execute data processing tasks. The UAV's position is denoted as $(x_{uav}, y_{uav}, z_{uav})$, and the USV_k's position is denoted as (x_k, y_k, 0). The distance between USV_k and UAV is represented as:

$$d_{k,uav} = \sqrt{\left(x_{uav} - x_k\right)^2 + \left(y_{uav} - y_k\right)^2 + z_{uav}^2} \tag{12}$$

the channel gain can be described using the free-space path loss model:

$$H_k = \frac{\chi}{d_{k,uav}^{\eta}} \tag{13}$$

where parameter χ is the channel power gain at a unit distance, and parameter η is the path loss exponent.

The data rate for uplink transmission between USV_k and the UAV can be represented as:

$$r_k = B_k \log_2\left(1 + \frac{p_k H_k}{N}\right) \tag{14}$$

where B_k is the allocated channel bandwidth allocated to USV_k, p_k is the transmit power of USV_k, N is the background noise power at USV_k.

2.3 Analysis of Latency and Energy Consumption

2.3.1 Latency

The USV_k's task completion latency includes both the data collection latency and the processing latency, that is:

$$t_k = t_k^{coll} + t_k^{proc} \tag{15}$$

The latency for $USN_{k,i}$ uploading collected data to USV_k is:

$$t_{k,i} = \frac{R_{k,i}}{r_{k,i}} \tag{16}$$

The underwater data collection latency of USV_k is:

$$t_k^{coll} = \max_{i \in \mathcal{I}} \left\{t_{k,i}\right\} \tag{17}$$

The amount of the processing data of USV_k is:

$$R_k = \sum_{i \in \mathcal{I}} R_{k,i} \tag{18}$$

where $R_{k,i}$ is the amount of data uploaded to USV_k from $USN_{k,i}$.

USV_k offloaded partial data to the UAV. Denote the offloading ratio as β_k. f_k representing the computing resources allocated to USV_k . The local processing latency of USV_k is:

$$t_k^{local} = \frac{(1-\beta_k)C_k}{F_k} \tag{19}$$

The latency for USV_k uploading to UAV is:

$$t_k^{up} = \frac{\beta_k R_k}{r_k} \tag{20}$$

The UAV's latency for computing the data from USV_k is:

$$t_k^{uav} = \frac{\beta_k C_k}{f_k} \tag{21}$$

The offloading latency t_k^{off} consists of two parts: the uploading latency t_k^{up} and the UAV's computation latency t_k^{uav}. Therefore, t_k^{off} can be represented as:

$$t_k^{off} = t_k^{up} + t_k^{uav} \tag{22}$$

Since the local processing and offloading to the UAV can occur simultaneously, the task processing latency t_k^{proc} is:

$$t_k^{proc} = \max\left\{t_k^{local}, t_k^{off}\right\} \tag{23}$$

2.3.2 Energy Consumption

The focus of this paper is primarily on the users' experience. Therefore, only the energy consumption generated by USVs is considered. The energy consumption includes both USV's computation energy consumption and USV's transmission energy consumption for data transmission. Due to the significant difference between received and transmit power levels, the energy consumed in transmitting results can generally be disregarded.

The local computation of USV_k results in computational energy consumption. The USV_k's computational energy consumption E_k^{local} can be represented as:

$$E_k^{local} = \alpha(1-\beta_k)C_k F_k^2 \tag{24}$$

where α is the energy factor of USVs, which is related to the CPU architecture of USVs.

The process of USV_k uploading data to the UAV incurs transmission energy consumption. The transmission energy consumption E_k^{trans} is represented as:

$$E_k^{trans} = \frac{\beta_k R_k}{r_k} p_k \tag{25}$$

The USV_k's total energy consumption comprises both E_k^{local} and E_k^{trans}. Therefore, the USV_k's total energy consumption E_k can be represented as:

$$E_k = E_k^{local} + E_k^{trans} \tag{26}$$

2.4 Optimization Problem

To enhance user's experience, this paper comprehensively considers both task completion latency and energy consumption of users. It aims to minimize the weighted sum of USV's latency and energy consumption. Thus, an optimization problem is formulated with this objective in mind:

$$\begin{aligned} P1: \quad & \min_{P_{k,i}, p_k, \beta_k B_k} V = \sum_{k\in\mathcal{K}} w_1 t_k + w_2 E_k \\ s.t. \quad & C1: \ 0 \le P_{k,i} \le P_i^{\max}, \forall i \in \mathcal{I} \\ & C2: \ 0 \le B_k \le B_{total}, \forall k \in \mathcal{K} \\ & C3: \ \sum_{k\in\mathcal{K}} B_k \le B_{total}, \forall k \in \mathcal{K} \\ & C4: \ 0 \le \beta_k \le 1, \forall k \in \mathcal{K} \\ & C5: \ 0 \le p_k \le p_k^{\max}, \forall k \in \mathcal{K} \end{aligned} \tag{27}$$

where w_1 represents the latency weighting factor, reflecting the importance users place on latency, and w_2 represents the energy consumption weighting factor, reflecting the importance users place on energy consumption. Constraint C1 specifies the upper and lower limits of the $USN_{k,i}$'s transmission power. Constraint C2 specifies the upper and lower limits of the bandwidth resource allocated to USV_k. Constraint C3 ensures that the total bandwidth resource allocated to USVs does not exceed its upper limit. Constraint C4 specifies the upper and lower limits of the offloading ratio for USV_k, and C5 specifies the upper and lower limits of the USV_k's transmission power.

It is noticeable that problem P1 is a mixed-integer programming problem, which complicates the direct attainment of the optimal solution. Let's discuss the USV_k's sum of latency and energy consumption and denote it using V_k. V_k consists of two parts: latency t_k and energy consumption E_k. latency t_k includes the data collection stage's latency t_k^{coll} and the data processing stage's latency t_k^{proc}, where $t_k^{coll} = \max_{i\in\mathcal{I}} \left\{ \frac{R_{k,i}}{r_{k,i}} \right\}$ and $t_k^{proc} = \max \left\{ \frac{(1-\beta_k)C_k}{F_k}, \frac{\beta_k R_k}{r_k} + \frac{\beta_k C_k}{f_k} \right\}$. Energy consumption E_k includes USV_k's computational energy consumption E_k^{local} while USV_k processing data locally and transmission energy consumption E_k^{trans} for transmitting data to UAV, where $E_k^{local} = \alpha(1-\beta_k)\, C_k F_k^2$ and $E_k^{trans} = \frac{\beta_k R_k}{r_k} p_k$. Thus, V_k can be represented as:

$$\begin{aligned} V_k = {} & w_1 \left(\max_{i\in\mathcal{I}} \left\{ \frac{R_{k,i}}{r_{k,i}} \right\} + \max \left\{ \frac{(1-\beta_k)C_k}{F_k}, \frac{\beta_k R_k}{r_k} + \frac{\beta_k C_k}{f_k} \right\} \right) \\ & + w_2 \left(\alpha(1-\beta_k) C_k F_k^2 + \frac{\beta_k R_k}{r_k} p_k \right) \end{aligned} \tag{28}$$

From (11), it is clear that t_k^{coll} in data collection stage is only influenced by $USN_{k,i}$'s transmission power $P_{k,i}$. From (14), t_k^{proc} and E_k in data processing stage are impacted by USV_k's bandwidth B_k, USV_k's offloading ratio β_k and USV_k's transmission power p_k. Besides, $P_{k,i}$'s constraint C1 is independent of constraints C2-C5. Thus, the data collection stage is independent of the data processing stage. To make the problem P1 more intuitive, we decompose P1 into two sequential subproblems: underwater data collection stage and on-water data processing stage, optimizing each stage separately.

In the underwater data collection stage, the optimization objective is to minimize the data collection latency of USVs, the optimization variable is the transmission power of USNs, and the optimization problem is formulated as:

$$\begin{aligned} P2: \quad & \min_{P_i} \sum_{i\in\mathcal{I}} t_k^{coll} \\ s.t. \quad & C1: \ 0 \le P_i \le P_i^{\max}, \forall i \in \mathcal{I} \end{aligned} \tag{29}$$

In the data processing stage, the optimization objective is to minimize the weighted sum of the data processing latency and energy consumption of USVs, the optimization variables are the USVs' transmission power $\boldsymbol{p}$, USVs' offloading ratio $\boldsymbol{\beta}$, and USVs' bandwidth $\boldsymbol{B}$, and the optimization problem is formulated as follows:

$$\begin{aligned} P3: \quad & \min_{p_k, f_k, \beta_k} \sum_{k\in\mathcal{K}} w_1 t_k^{proc} + w_2 E_k \\ s.t. \quad & C2: \ 0 \le B_k \le B_{total}, \forall k \in \mathcal{K} \\ & C3: \ \sum_{k\in\mathcal{K}} B_k \le B_{total}, \forall k \in \mathcal{K} \\ & C4: \ 0 \le \beta_k \le 1, \forall k \in \mathcal{K} \\ & C5: \ 0 \le p_k \le p_k^{\max}, \forall k \in \mathcal{K} \end{aligned} \tag{30}$$

By sequentially obtaining the optimal solution to problems P2 and P3, the original problem P1 can be solved, and the minimum weighted sum of USV's latency and energy consumption can be found.

3 Problem Solution

3.1 The Data Collection Stage

Since the data collection latency of USVs is independent of each other, minimizing the collection latency of a single USV will result in minimizing the total collection latency. Without loss of generality, discuss the optimization problem of the collection latency of the kth USV:

$$\begin{aligned} P4: \quad & \min_{P_{k,i}} t_k^{coll} = \max_{i\in\mathcal{I}} \{ t_{k,i} \} \\ s.t. \quad & C1: \ 0 \le P_{k,i} \le P_i^{\max}, \forall i \in \mathcal{I} \end{aligned} \tag{31}$$

Under the constraint of limited communication resources, sensors' data needs to arrive simultaneously to minimize the data collection latency. Therefore, problem P2 is transformed into optimizing the transmit power to ensure that the data arrival time at the kth USV is equal. This paper employs a particle swarm optimization (PSO) algorithm to solve this problem.

Derived from the behavior of birds when foraging, the PSO algorithm operates on the principle of information sharing and collaborative screening among individuals within a population to discover the optimal solution. In this paper, a population consists of N particles (also referred to as individuals), each particle having two attributes: position and velocity. The position of each particle represents a transmission power scheme of the USNs, while the velocity represents the evolution process of the transmission power scheme. Both position and velocity have dimensions equal to the number of USNs. The position and velocity of the nth particle are represented as follows:

$$\boldsymbol{X}_n = \left(X_{n1}, \cdots, X_{ni}, \cdots, X_{nI}\right) \tag{32}$$

$$\boldsymbol{v}_n = \left(v_{n1}, \cdots, v_{ni}, \cdots, v_{nI}\right) \tag{33}$$

During the search process, each particle X_n^t updates its new position X_n^{t+1} based on its velocity V_n^{t+1}. The velocity and position updates for each particle are as follows:

$$\begin{aligned}\boldsymbol{v}_n^{t+1} &= \omega \cdot \boldsymbol{v}_n^t + c_1 \cdot r_1 \cdot \left(\boldsymbol{pbest}_n^t - \boldsymbol{X}_n^t\right) \\ &+ c_2 \cdot r_2 \cdot \left(\boldsymbol{gbest}^t - \boldsymbol{X}_n^t\right)\end{aligned} \tag{34}$$

$$\boldsymbol{X}_n^{t+1} = \boldsymbol{X}_n^t + \boldsymbol{v}_n^{t+1} \tag{35}$$

where ω is the inertia weight, c_1 and c_2 are the learning factors, commonly referred to as social confidence or cognitive confidence. r_1 and r_2 are random numbers between [0,1]. $\boldsymbol{pbest}_n^t$ is the historical best position of the nth particle, and $\boldsymbol{gbest}^t$ is the historical best position of the population.

Using PSO algorithm to maximize the fitness function enables the determination of the optimal transmission power scheme for USNs. In order to solve problem P4, the collection latency of USV_k is constructed as a part of the fitness function. To simplify the solution, the constraint C1 is incorporated into the objective function (30) using penalty function method.

The fitness function of the particles is constructed as follows:

$$F\left(\boldsymbol{X}\right) = R - \max_{i \in \mathcal{I}} \left\{t_{k,i}\right\} - P\left(\boldsymbol{X}\right) \tag{36}$$

where R is a constant ensuring that the fitness function value is positive, and $P(\boldsymbol{P})$ is the penalty function defined as:

$$P\left(\boldsymbol{X}\right) = \sum_{i \in \mathcal{I}} \lambda \max\left\{0, P_i^{\max} - X_i\right\} \tag{37}$$

where parameter λ is the penalty factor, which is a positive number. During the process of uploading data from USNs to the USV, each USN's transmit power is compared with the maximum power value. If it exceeds the maximum value, it will be penalized through the penalty function, increasing the fitness of the particle accordingly. If it does not exceed the maximum value, the penalty function is 0, indicating no penalty is applied.

The optimization algorithm for USN's transmission power proceeds as described in Algorithm 1. Firstly, a set of particle populations is initialized, with each particle having an initial position and velocity. The fitness function value is calculated based on equation (36), marked as the current individual's historical best solution. Then, through collaborative information sharing among particles, the global historical best solution is obtained, and new velocities and positions are iteratively computed. Subsequently, the fitness function value of the particles' new positions is calculated. If the new fitness function value is greater than the particle's previous historical best solution, then this new fitness function value becomes the particle's new historical best solution. After updating all particles' historical best solutions, the global historical best solution is updated, and the iteration continues until convergence of the algorithm.

Algorithm 1. Particle swarm optimization algorithm for transmit power control of USNs

1. **Initialization**
2. Population Size N, Particle Positions $\boldsymbol{X}$, Particle Velocities $\boldsymbol{v}$, Maximum Iteration Count $t^{\max}$
3. t=1;
4. **While** $t < t^{\max}$ do
5. **For** n=1 to N
6. Update the velocity and position of particle n
7. Calculate the fitness of particle n at this time according to Equation (35).
8. If $F(X_n^t) > F(\boldsymbol{pbest}_n^t)$
9. $\boldsymbol{pbest}_n^t = \boldsymbol{X}_n^t$;
10. If $F(\boldsymbol{pbest}_n^t) > F(\boldsymbol{gbest}^t)$
11. $\boldsymbol{gbest}^t = \boldsymbol{pbest}_n^t$;
12. **End For**
13. t=t+1；
14. **End While**
15. **Output** the position of the particle with the highest fitness in the population as the optimal transmission power scheme $\{\boldsymbol{P}^*\}$

3.2 The Data Processing Stage

In the optimization problem P3 during the data processing stage, the objective function involves coupled variables, making it an NP-hard problem that is tough to obtain its optimal solution directly. Therefore, it is decomposed into three sub-problems: USVs' transmission power control, USVs' offloading strategy, and USVs' bandwidth allocation. Each sub-problem is solved using gradient descent, genetic algorithm, and CVX algorithm, respectively, and then the solutions are obtained through alternating iterations to solve the entire problem.

3.2.1 USV's Transmission Power Optimization

According to (20), it can be observed that the USV's transmission power variables ***p*** are independent of each other. Thus, the transmission power parameters for individual USVs can be optimized independently. As transmission power only affects data upload latency and transmission energy consumption, when bandwidth allocation and offloading strategies are determined, the USV_k's power optimization problem can be represented as:

$$\begin{aligned} P5:\ &\min_{p_k}\ w_1 t_k^{proc} + w_2 E_k^{trans} \\ s.t.\ &C5:\ 0 \le p_k \le p_k^{\max}, \forall k \in \mathcal{K} \end{aligned} \tag{38}$$

where $t_k^{proc} + E_k^{trans} = w_1 \max\left\{t_k^{local}, t_k^{off}\right\} + w_2 \dfrac{\beta_k R_k}{r_k} p_k$.

When the bandwidth allocation and offloading strategy are determined, setting the transmission power to its maximum value $p_k^{\max}$ can achieve the maximum transmission rate $r_k^{\max}$, and the latency of offloading to UAV reaches its minimum value t_k^{off}, represented as:

$$t_{k,\min}^{off} = \frac{\beta_k R_k}{r_k^{\max}} + \frac{\beta_k C_k}{f_k} \tag{39}$$

where $r_k^{\max} = B_k \log_2\left(1 + \dfrac{p_k^{\max} H_k}{N_k}\right)$.

Let $Q_k = w_1 t_k^{proc} + w_2 E_k^{trans}$, and analyze the two cases separately: when the local latency is greater than $t_{k,\min}^{off}$ and when the local latency is less than $t_{k,\min}^{off}$.

(1) When $t_k^{local} < t_{k,\min}^{off}$, the first-order partial derivative of Q_k with respect to p_k is:

$$\frac{\partial Q_k}{\partial p_k} = \beta_k R_k \frac{\ln 2}{B_k}\left[\frac{w_2\left(\ln(1+S_k) - \dfrac{S_k}{1+S_k}\right) - w_1 \dfrac{S_k}{(1+S_k)p_k}}{(\ln(1+S_k))^2}\right] \tag{40}$$

where S_k is the signal-to-noise ratio, and $S_k = \dfrac{p_k H_k}{N_k}$.

Let $\dfrac{w_1 S_k}{p_k}$ be denoted by constant A. Equation (39) can be rewritten as:

$$\frac{\partial Q_k}{\partial P_k} = \beta_k R_k \frac{\ln 2}{B_k}\left[\frac{w_2\left(\ln(1+S_k) - \dfrac{S_k}{1+S_k}\right) - \dfrac{A}{(1+S_k)}}{(\ln(1+S_k))^2}\right] \tag{41}$$

Let $f(S_k) = w_2\left(\ln(1+S_k) - \dfrac{S_k}{1+S_k}\right) - \dfrac{A}{(1+S_k)}$, when $S_k = 0, f(S_k) < 0$.

$$\frac{\partial f}{\partial S_k} = \frac{A}{(1+S_k)^2} + \frac{w_2 S_k}{(1+S_k)^2} \ge 0 \tag{42}$$

From equation (41), it is clear that $f(S_k)$ is a monotonically increasing function. Because p_k and S_k are directly proportional, $f(p_k)$ is also a monotonically increasing function. If there does not exist p_k in the interval $[0, p_k^{\max}]$ can make $f(S_k) > 0$, then Q_k is monotonically decreasing in this interval, and Q_k takes its minimum value when $p_k = p_k^{\max}$; if there exists p_k can make $f(S_k) > 0$, then Q_k decreases first and then increases in the interval $[0, p_k^{\max}]$, there exists $\overline{p}_k$ such that $f(\overline{p}_k) = 0$ and Q_k takes its minimum value when $p = \overline{p}_k$. In summary, the minimum value of Q_k is either obtained at points where the derivative is zero or at the larger boundary of the transmission power.

Let $p_k(1) = p_k^{\max}$. If $\dfrac{\partial Q_k(1)}{\partial p_k(1)} \le 0$, it is clear that Q_k is monotonically decreasing in the domain, and $p_k^* = p_k^{\max}$. If $\dfrac{\partial Q_k(1)}{\partial p_k(1)} \ge 0$, Q_k first decreases and then increases in the domain. Utilize gradient descent method to find the minimum value point where the derivative equals zero, and the step update formula for gradient descent is:

$$p_k(t+1) = p_k(t) - v\frac{\partial Q_k(t)}{\partial p_k(t)} \tag{43}$$

Update p_k using formula (42), stop updating when $\dfrac{\partial Q_k(t)}{\partial p_k(t)} \approx 0$, and $p_k^* = p_k(t)$.

(2) When $t_k^{local} \ge t_{k,\min}^{off}$, there exists a valid power $\dot{p}_k$ such that the local computation latency of USV_k is equal to the latency of offloading to UAV.

Let $\dfrac{(1-\beta_k)C_k}{F_k} = \dfrac{\beta_k R_k}{r_k} + \dfrac{\beta_k C_k}{f_k}$, $\dot{p}_k = \left(2^{V_k} - 1\right)\dfrac{N_k}{H_k}$,

where $V_k = \dfrac{\beta_k R_k}{B_k\left[\dfrac{(1-\beta_k)C_k}{F_k} - \dfrac{\beta_k C_k}{f_k}\right]}$.

Represent the data processing latency of USV_k at this moment as:

$$t_k^{proc} = \begin{cases} \dfrac{\beta_k R_k}{r_k} + \dfrac{\beta_k C_k}{f_k}, 0 \le p_k \le \dot{p}_k \\ \dfrac{(1-\beta_k)C_k}{F_k}, \dot{p}_k \le p_k \le \mathrm{p}_k^{\max} \end{cases} \tag{44}$$

When $0 \le p_k \le \dot{p}_k$. From equations (41) and (42), if Q_k is monotonically decreasing in the domain, then the minimum value is attained at the transmission power's larger boundary point $\dot{p}_k$; If Q_k first decreases and then increases in the domain, then the minimum value is attained at the point $\overline{p}_k$ where the derivative equals zero.

When $\dot{p}_k \le p_k \le p_k^{\max}$. The first-order derivative of Q_k is:

$$\frac{\partial Q_k}{\partial P_k} = \beta_k R_k \frac{\ln 2}{B_k} \left[\frac{w_2 \left(\ln(1+S_k) - \dfrac{S_k}{1+S_k} \right)}{(\ln(1+S_k))^2} \right] \quad \textbf{(45)}$$

Let $f(S_k) = \ln(1+S_k) - \dfrac{S_k}{1+S_k}$, and $f(S_k) = 0$ when $S_k = 0$.

$$\frac{\partial f}{\partial S_k} = \frac{S_k}{(1+S_k)^2} \ge 0 \quad \textbf{(46)}$$

The first-order derivative of Q_k with respect to S_k is non-negative in its domain, indicating that Q_k is monotonically increasing with respect to S_k. Moreover, since p_k is positively correlated with S_k, Q_k is a monotonically increasing function of p_k. The minimum value of Q_k is obtained at the smaller boundary value $\dot{p}_k$, and $p^* = \dot{p}_k$.

The optimization process of USV's transmission power is illustrated in Algorithm 2. Under the current decision of offloading ratio and the magnitude of the signal-to-noise ratio, the minimum data offloading latency $t_{k,\min}^{off}$ can be computed. When the offloading latency $t_{k,\min}^{off}$ is greater than the local computation latency, compute the partial derivative of Q_k at $p_k^{\max}$. If the derivative is greater than 0, indicating the existence of a point $\overline{p}_k$ where the derivative equals 0, the minimum value is attained at $\overline{p}_k$. Otherwise, it is attained at $p_k^{\max}$; When the local latency is greater than $t_{k,\min}^{off}$, compute the partial derivative of Q_k at $\dot{p}_k$. If the derivative at this point is greater than 0, indicating the existence of a point $\overline{p}_k$ where the derivative equals 0, the minimum value is attained at $\overline{p}_k$. Otherwise, it is attained at $\dot{p}_k$.

Algorithm 2. USV's transmission power optimization algorithm

1. **Input** offloading ratio decision $\{\boldsymbol{\beta}\}$, signal-to-noise ratio $\{\boldsymbol{S}\}$, and calculate $\{t_{\min}^{off}\}$.
2. **If** $t_k^{local} < t_{k,\min}^{off}$
3. $p_k(1) = p_k^{\max}$
4. **If** $\dfrac{\partial Q_k(1)}{\partial p_k(1)} \le 0$
5. $p_k^* = p_k^{\max}$
6. **Else**
7. Search for the optimal point $\overline{p}_k$ according to the step update equation (42)
8. $p_k^* = \overline{p}_k$
9. **End If**
10. **End If**
11. **If** $t_k^{local} \ge t_{k,\min}^{off}$
12. $p_k(1) = \dot{p}_k$
13. **If** $\dfrac{\partial Q_k(1)}{\partial p_k(1)} \le 0$
14. $p_k^* = \dot{p}_k$
15. **Else**
16. Search for the optimal point according to $\overline{p}_k$ the step update equation (42)
17. $p_k^* = \overline{p}_k$
18. **End If**
19. **End If**
20. **Output** the USV's optimal transmission power decision $\{\boldsymbol{p}^*\}$

3.2.2 USV's Bandwidth Allocation Optimization

According to equations (20), (21), and (25), it is evident that the bandwidth allocation scheme only affects the USV's transmission latency and transmission energy consumption. Therefore, when the USV's transmission power and offloading strategy are determined, the bandwidth resource allocation sub-problem is as follows:

$$\begin{aligned} P6:\ & \min_{B_k} \sum_{k\in\mathcal{K}} w_1 \frac{\beta_k R_k}{r_k} + w_2 \frac{\beta_k R_k}{r_k} p_k \\ & s.t.\ C2:\ 0 \le B_k \le B_{total}, \forall k \in \mathcal{K} \\ & \qquad C3:\ \sum_{k\in\mathcal{K}} B_k \le B_{total}, \forall k \in \mathcal{K} \end{aligned} \quad \textbf{(47)}$$

Let $G(\boldsymbol{B})$ denote the objective function, and $G(\boldsymbol{B})$ is represented as:

$$z\, G(\boldsymbol{B}) = \sum_{k\in\mathcal{K}} w_1 \frac{Y_k}{B_k} + w_2 \frac{Y_k}{B_k} p_k \quad \textbf{(48)}$$

where Y_k is a constant and $Y_k = \dfrac{\beta_k R_k}{\log_2\left(1 + \dfrac{p_k H_k}{N_k}\right)}$.

Hessian matrix of the objective function $G(\boldsymbol{B})$ can be represented as:

$$H = \begin{bmatrix} \dfrac{\partial^2 G}{\partial B_1^2} & \cdots & \dfrac{\partial^2 G}{\partial B_1 \partial B_K} \\ \vdots & \ddots & \vdots \\ \dfrac{\partial^2 G}{\partial B_K \partial B_1} & \cdots & \dfrac{\partial^2 G}{\partial B_K^2} \end{bmatrix} \quad \textbf{(49)}$$

Without loss of generality, for USV_k, the second-order partial derivative of $G(\boldsymbol{B})$ with respect to B_k is:

$$\frac{\partial^2 G}{\partial B_k^2} = \left(w_1 + w_2 p_k\right)\frac{2Y_k}{B_k^3} \geq 0 \tag{50}$$

The mixed second-order partial derivatives of $G(\boldsymbol{B})$ with respect to the bandwidth of other USVs are:

$$\frac{\partial^2 G}{\partial B_k \partial B_o} = 0, \forall o \in \mathcal{K}, o \neq k \tag{51}$$

According to equations (49) and (50), we can determine that H is a positive definite matrix, $G(\boldsymbol{B})$ is convex, and the feasible domain set formed by constraints C2 and C3 is convex. Therefore, problem P6 is a convex problem. Address problem P6 by utilizing MATLAB's built-in CVX toolbox.

3.2.3 USV's Offloading Decision Optimization

The optimization sub-problem of offloading strategy can be represented once the transmission power and bandwidth allocation are determined:

$$\begin{aligned} P7\text{:} \ & \min_{\beta_k} \sum_{k\in\mathcal{K}} w_1 \cdot t_k^{proc} + w_2 E_k \\ & s.t. \ \ C4\text{: } 0 \leq \beta_k \leq 1, \forall k \in \mathcal{K} \end{aligned} \tag{52}$$

The objective function is a maximum value function concerning the offloading ratio. Since the maximum value function is not differentiable, traditional gradient descent methods cannot be used. Genetic Algorithm (GA) is an optimization method that mimics the biological process of genetic evolution. It can directly manipulate the optimization objects, thereby overcoming the limitations of traditional search methods on the differentiability of the objective function. Therefore, this paper adopts the genetic algorithm to attain the optimal offloading ratio strategy vector $\boldsymbol{\beta}$.

GA maps the solution vector of the optimization problem into each individual in the genetic space population, and then performs operations such as mutation and crossover on the genes on the chromosome of each individual, following the law of survival of the fittest to iteratively screen out excellent individuals in the population. In this paper, a populati $H = \begin{bmatrix} \frac{\partial^2 G}{\partial B_1^2} & \cdots & \frac{\partial^2 G}{\partial B_1 \partial B_K} \\ \vdots & \ddots & \vdots \\ \frac{\partial^2 G}{\partial B_K \partial B_1} & \cdots & \frac{\partial^2 G}{\partial B_K^2} \end{bmatrix}$ on consists of $\tilde{U}$ individuals, and each individual has K chromosomes. The process of expressing chromosomes as genes is called encoding, and the offloading ratio β_k is encoded and mapped to the gene value on the chromosome. Considering that the offloading ratio β_k is a continuous variable, this paper adopts floating-point encoding as the encoding method. Floating-point encoding means using a floating-point number within a specific interval to represent the individual's gene value. After floating-point encoding, there is one gene value on each chromosome. Denote and the gene value vector of the uth individual as $\boldsymbol{\beta}_u = \{\beta(u, 1), ..., \beta(u, k), ..., \beta(u, K)\}$, where $\beta(u, k)$ represents the offloading ratio of the kth gene value on the uth individual.

GA uses the fitness function value to evaluate the goodness or badness of an individual. The larger the fitness value, the smaller the overall cost calculated by the offloading decision solution, indicating that the solution is better. By eliminating chromosomes with lower fitness and retaining those with higher fitness, the algorithm can gradually approach the optimal solution. The fitness function of this paper's genetic algorithm is set as follows:

$$F\left(\boldsymbol{\beta}\right) = T - \sum_{k\in\mathcal{K}}\left(w \cdot t_k^{mec} + E_k\right) \tag{53}$$

where T is a constant, ensuring that the fitness function value is positive.

The optimization process of the USVs' offloading ratio is shown in Algorithm 3. In the initialization phase, the relevant parameters are initialized firstly, including the population size $\tilde{U}$, the maximum number of genetic evolutions $\tilde{i}$, the individual mutation probability $\tilde{m}$, the crossover probability $\tilde{a}$, and the number of eliminated individuals in each round $\tilde{z}$. After the initialization phase is completed, the algorithm begins the iteration process. In each evolutionary round of the population, mutation and crossover operations are performed. In evolutionary round tau, the following mutation operation is performed on each individual: for each gene on the individual, a random number between [0,1], denoted as $rand^m$, is generated. If $rand^m$ is less than $\tilde{m}$, then the mutation operation is applied to that gene. Let (u, k) denote the mutation position, the mutation expression is given by:

$$\beta'\left(u,k\right) = \beta(u,k) \cdot \left(1 \pm \frac{rand}{(1-\frac{tau}{\tilde{i}})^2}\right) \tag{54}$$

For each individual, the following crossover operation is performed: a random number $rand^a$ is generated between [0,1]. If $rand^a$ is less than $\tilde{a}$, the individual undergoes a crossover operation. Randomly select the gene on this individual, denoting its position as (u, k), then randomly select a gene at position (u^a, k^a) in the population, and let $\beta'(u, k) = \beta(u^a, k^a)$.

After performing mutation and crossover operations on each individual in the population, the selection phase is entered. The current best individual in the iteration round is found based on the fitness of each individual, and it replaces the previously stored best individual. At the same time, some inferior individuals in the population are replaced with the best individual to generate the initial population for the next evolution. When the algorithm reaches the maximum iteration round, the optimal offloading decision vector $\{\boldsymbol{\beta}^*\}$, which is the individual with the highest fitness in the population at that time, is output.

Algorithm 3. Offloading decision optimization algorithm

1. **Input** population size $\tilde{U}$, number of generations $\tilde{i}$, mutation probability $\tilde{m}$, crossover probability $\tilde{a}$, and number of individuals eliminated per round $\tilde{z}$
2. **Initialize** the genetic values of the population individuals and calculate the initial fitness function values
3. tau=1
4. **While** $tau < \tilde{i}$ **do**
5. Perform crossover and mutation operations on individuals in the current population
6. Recalculate the fitness of individuals
7. Find new optimal individuals and replace the stored optimal individual
8. Replace the top $\tilde{z}$ individuals with the optimal individual, where $\tilde{z}$ is the specified number
9. $tau = tau + 1$
10. **End While**
11. **Output** the individual with the highest fitness in the evolved population as the optimal task offloading decision $\{\boldsymbol{\beta}^*\}$

In summary, the entire optimization algorithm for computation offloading and resource allocation in OMNs first decomposes problem P1 into two subproblems: the data collection stage problem P2 and the data processing stage problem P3. The optimization problem P2 enables collected data to arrive at the USV simultaneously by using the particle swarm optimization algorithm to control the USN's transmission power. The optimization problem P3 is decomposed into three sub-problems: the USV's transmission power, USV's offloading decision, and USV's bandwidth allocation, which are optimized separately by using gradient descent, genetic algorithm, and CVX solver respectively.

Complexity is a key factor to assess the practicability of an algorithm, hence it is necessary to analyze the complexity of the proposed algorithms. First, analyze the complexity of Algorithm 1. Algorithm 1 uses PSO, with N particles in the swarm, a search space dimension of I, and a maximum number of iterations $t_{\max}$. Therefore, the complexity of Algorithm 1 is O(NI $t_{\max}$). Algorithm 2 uses gradient descent. Since the iteration process of gradient descent is influenced by the step size, it is difficult to provide a direct complexity. Assuming that Algorithm 2 requires T iterations to converge, the complexity of Algorithm 2 is O(TK). Algorithm 3 uses a genetic algorithm, with $\tilde{U}$ chromosomes, $\tilde{i}$ iterations, and a search space dimension of K. Therefore, the complexity of Algorithm 3 is O($\tilde{U}\,\tilde{i}$ K). Since each iteration requires executing Algorithm 2 and Algorithm 3 once and needs $y_{\max}$ iterations, the overall complexity of the entire algorithm is O($y_{\max}$ TK)+O($y_{\max}$ $\tilde{U}\,\tilde{i}$ K)+ O(NI $t_{\max}$).

4 Simulation and Analysis

This paper utilizes MATLAB to simulate the proposed algorithm in order to validate its effectiveness. It is assumed that the positions of USNs are randomly generated. The amount of data uploaded by each USN is 1kb. The UAV's flight altitude is set to 200m. The channel fading between the USVs and the UAV is calculated based on the large-scale fading model $H_k = \chi d_{k,uav}^{-\lambda}$, where χ represents the channel fading coefficient, $d_{k,uav}$ represents the spatial distance between the communication nodes (USVs) and UAV, and λ represents the channel fading exponent. Other relevant parameters are as shown in the Table 2 below.

Table 2. Simulation parameters

Parameters	Values
Shipping activity factor, a	0.5
Wind speed, b	5m/s
Spreading factor, γ	1.5
Center frequency of the acoustic signal, θ	1Khz
Channel power gain χ	10^{-4}
Processing capability of USV_k, F_k	10MHz
Processing capability of UAV, F_{uav}	1Ghz
Upper limit of USN's transmission power, $P_i^{\max}$	0.1W
Task complexity, κ	1000cycle/bit
White noise power at USNs, σ^2	-100dBm
Bandwidth of USNs, B_{usn}	10KHZ
Amount of data uploaded by each USN	1Kbit
Total bandwidth allocated to USVs, B_{total}	1MHz
Energy factor of USVs, α	0.5×10^{-25}
Latency weighting factor, w_1	1
Energy consumption weighting factor, w_2	5
Background noise power at US_Vk	-100dBm
Upper limit of USV's transmission power, $p_k^{\max}$	3W

Figure 3 illustrates the convergence characteristics of the four algorithms when the number of USVs is 3. (a) shows that Algorithm 1 can converge within sixty iterations. (b) shows that Algorithm 2 can converge within ten iterations. (c) shows that Algorithm 3 can converge within thirty iterations. (d) shows that Algorithm 4 can converge within twenty iterations. The optimization objective values of Algorithms 1, 2, 3, and 4 all decrease as the number of iterations increases before reaching the convergence state and remain stable after convergence, demonstrating the validity of the four algorithms.

In order to validate the effectiveness of the algorithm introduced in this paper, it is contrasted with five other algorithms for comparison. Bandwidth average algorithm evenly distributes bandwidth resources, with optimization of other parameters similar to the method outlined in this paper. In max-pk algorithm, the USV's transmission power is adjusted to its upper limit $p_k^{\max}$, with optimization of other parameters similar to the method outlined in this paper. In fixed offloading algorithm, the USV's offloading ratio $\beta_k = 0.5$, with optimization of other parameters similar to the method outlined in this paper. In max-Pki algorithm, the USN's transmission power is adjusted to its upper limit $p_i^{\max}$, with optimization of other parameters similar to the method outlined in this paper. Algorithm of [17] adopts the optimization method from [17], which optimizes the offloading ratio under the conditions of user bandwidth averaging and fixed transmission power.

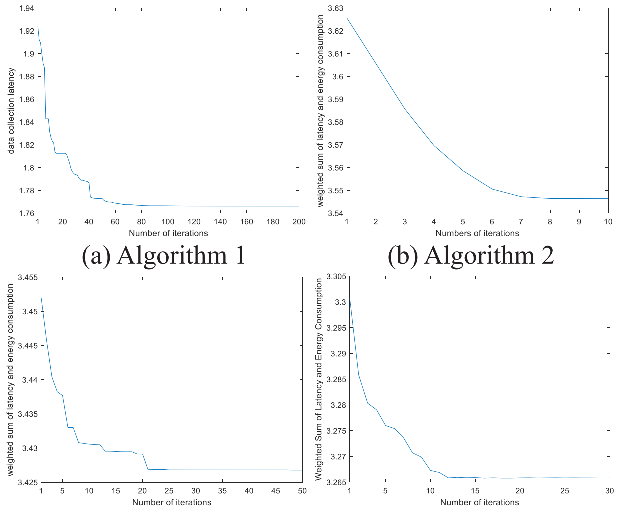

(a) Algorithm 1 (b) Algorithm 2

(c) Algorithm 3 (d) Algorithm 4

Figure 3. Convergence characteristics of algorithms

Algorithm 4. Entire optimization algorithm

---

1. **Input** the channel gain $\{\boldsymbol{g}_{k,i}\}$, USV's computing resources $\{\boldsymbol{f}\}$, and UAV's computing resources F_k
2. Execute Algorithm 1 to obtain the optimal transmission power scheme $\{\boldsymbol{P}^*\}$ for USNs
3. Calculate t_k^{coll}
4. y=1
5. **For** $y < y_{\max}$
6. y=y+1
7. Input $\{\boldsymbol{p}(y-1)\}$, $\{\boldsymbol{B}(y-1)\}$ and $\{\boldsymbol{\beta}(y-1)\}$
8. Execute Algorithm 2 to obtain transmission power decision $\{\boldsymbol{p}(y)\}$ for USNs
9. Use CVX to obtain bandwidth allocation $\{\boldsymbol{B}(y)\}$
10. Execute Algorithm 3 to obtain the optimal task offloading decision $\{\boldsymbol{\beta}(y)\}$
11. **End for**
12. **Output** optimal transmission power scheme $\{\boldsymbol{P}^*\}$, transmission power decision $\{\boldsymbol{p}^*\}$, bandwidth allocation $\{\boldsymbol{B}^*\}$ and task offloading decision $\{\boldsymbol{\beta}^*\}$

Figure 4 illustrates the performance contrast between the proposed algorithm and other algorithms across varying numbers of USVs when the latency weighting factor $w_1 = 1$ and the energy consumption weighting factor $w_2 = 5$. From Figure 4, it is clear that the number of USVs and the sum of USV's latency and energy consumption are positively correlated. This happens because the more USVs there are, the less bandwidth can be assigned to each USV, as the total bandwidth resources are limited, resulting in longer data transmission latency to the UAV. Additionally, the limited computing resources of the UAV and the increase in the total number of USVs result in a smaller amount of data that can be offloaded by each USV, leading to increased local computation workload and energy consumption.

Bandwidth average algorithm, max-pk algorithm and fixed offloading algorithm represent the performance of the three parameters separately without optimization in the data processing stage. It can be observed that contrast fixed offloading algorithm performs the worst, indicating that optimizing the offloading ratio provides the greatest performance gain. This is because in fixed offloading algorithm, the offloading ratio is a fixed constant (0.5), which cannot make the optimal offloading ratio decision based on the differences in channel gains between USVs. The offloading ratio affects the computation latency, transmission latency, local computation energy consumption, and transmission energy consumption. A fixed offloading ratio will result in wasted computing resources, leading to an increase in latency and energy consumption. Max-pk algorithm performs best, indicating that optimizing the transmission power of USVs provides the smallest performance gain. This is because transmits signals at maximum power in max-pk algorithm, resulting in the minimum data upload latency, but transmitting signals at maximum power may lead to an increase in energy consumption. Therefore, while max-pk algorithm lags behind the proposed algorithm in this paper, it outperforms other algorithms.

Compared with max-Pki algorithm, the proposed algorithm significantly reduces latency and energy consumption. This is because in max-Pki algorithm, the power of USNs is set to the its maximum value $P_i^{\max}$, ignoring the characteristics of NOMA channels, which reduces the signal-to-noise ratio of the acoustic channel, thus increasing the data collection latency of unmanned vessels. Compared with Algorithm of [17], the proposed algorithm performs better in reducing USV's latency and energy consumption. This is because [17] only optimizes the offloading ratio without optimizing bandwidth and transmission power. The strategy of uniformly allocating bandwidth ignores the differences in user channel environments, leading to wasted bandwidth resources. Fixed transmission power sizes cannot comprehensively consider latency and energy consumption, resulting in larger values of latency and energy consumption.

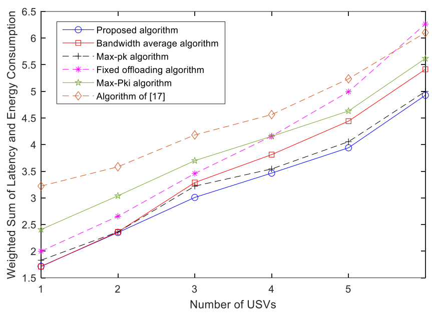

Figure 4. Performance comparison of the proposed algorithm and other algorithms

Figure 5 demonstrates how algorithm's performance is affected by varying numbers of USNs.

There exhibits a positive correlation between the number of USNs and the sum of USV's latency and energy consumption. As more USNs are deployed, the demand for data processing by USVs and UAVs also escalates. However, since communication and computation resources are limited, this leads to increases in data upload latency, computation latency, and energy consumption.

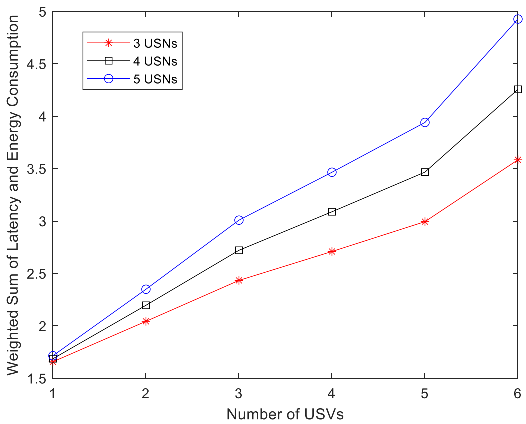

Figure 5. The impact of the number of USNs on the algorithm's performance

Figure 6 depicts the influence of total bandwidth on the algorithm's performance, with each USN collecting 1kb of data. it can be seen that as the total bandwidth increases, the weighted sum of latency and energy consumption decreases. This is because when the total bandwidth increases, the transmission rate also increases, resulting in reduced data upload latency and transmission energy consumption.

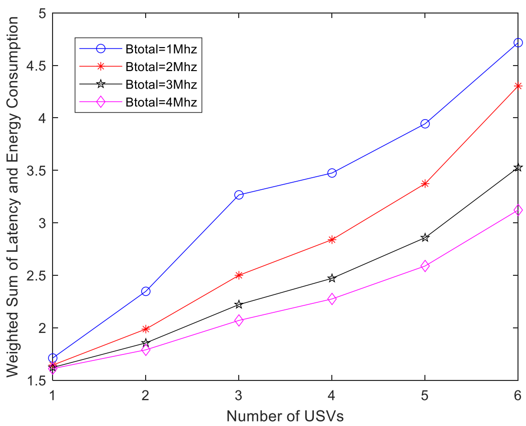

Figure 6. The influence of total bandwidth on the algorithm's performance

Figure 7 illustrates the influence of task computational complexity for USVs. From Figure 7, the impact of computational complexity on algorithm performance is not significant when there are only a few USVs. This is because the UAV's computational resources are sufficient at this moment, and USVs are more inclined to offload processing. Due to the strong computational capabilities of the UAV, the computational complexity has little effect on the processing latency of the UAV. However, with the growing number of USVs, the computational complexity begins to exert a more pronounced effect on algorithm performance. Additionally, as the number of USVs increases, the proportion of local computation also increases. The increase in computational complexity leads to an increase in the processing latency of local computation on USVs, thereby resulting in an increase in the weighted sum of latency and energy consumption.

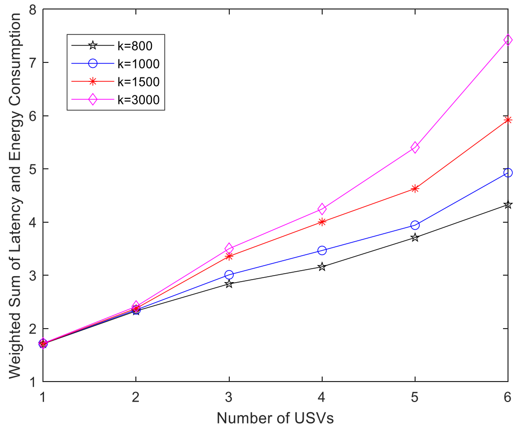

Figure 7. The influence of task computational complexity on the algorithm's performance

Figure 8 depicts the influence of USV's processing capability on the algorithm's performance. From Figure 8, it can be observed that when the processing capability of USVs is 10MHz, the performance is the best. This is because the processing capability of USVs only affects the local computation latency and local computation energy consumption. When the offloading ratio is determined, the first derivative of the weighted sum of local computation latency and energy consumption with respect to the processing capability of USVs has a unique stationary point. 10MHz is near this stationary point. When the processing capability of USVs is 5MHz, the local processing latency increases, leading to an increase in the overall energy consumption and latency. When the processing capability of USVs is 20MHz, the energy consumption of USVs increases, resulting in an increase in the overall energy consumption and latency.

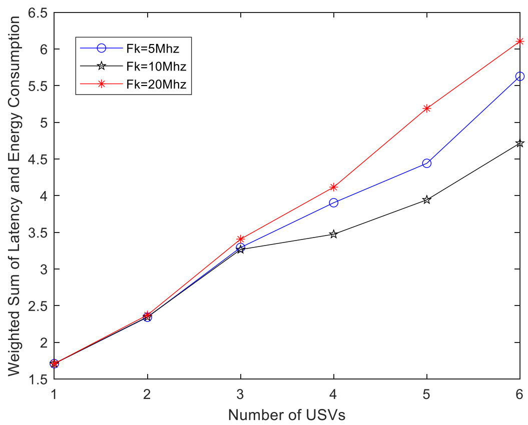

Figure 8. The influence of USV's computing capability on the algorithm's performance

5 Conclusion

In this paper, a computational offloading model for maritime monitoring networks was constructed using a hybrid NOMA and FDMA approach in a multi-USVs scenario. The weighted sum of latency and energy consumption during data collection and data processing stages of USVs was analyzed separately. The particle swarm optimization algorithm is employed to optimize the USN's transmission power. The offloading ratio, transmission power, and bandwidth allocation of USVs optimized using genetic algorithm, gradient descent algorithm, and CVX, respectively. Finally, MATLAB simulation was employed to validate the proposed algorithms. Simulation results demonstrate that the algorithms presented in this paper effectively reduce the weighted sum of latency and energy consumption for USVs.

Acknowledgement

This work is supported by Jiangsu Provincial Key Research and Development Program (No. BE2022068-2), the National Natural Science Foundation of China (No. 92367302).

References

[1] J. Wen, J. Yang, W. Wei, Z. Lv, Intelligent Multi-AUG Ocean Data Collection Scheme in Maritime Wireless Communication Network, *IEEE Transactions on Network Science and Engineering*, Vol. 9, No. 5, pp. 3067-3079, September-October, 2022. https://doi.org/10.1109/TNSE.2022.3164587

[2] Y. Fu, Y. Shan, Q. Zhu, K. Hung, Y. Wu, T. Q. S. Quek, A Distributed Microservice-aware Paradigm for 6G: Challenges, Principles, and Research Opportunities, *IEEE Network*, Vol. 38, No. 3, pp. 163-170, May, 2024. https://doi.org/10.1109/MNET.2023.3321528

[3] T. Wei, W. Feng, Y. Chen, C.-X. Wang, N. Ge, J. Lu, Hybrid Satellite-Terrestrial Communication Networks for the Maritime Internet of Things: Key Technologies, Opportunities, and Challenges, *IEEE Internet of Things Journal*, Vol. 8, No. 11, pp. 8910-8934, June, 2021. https://doi.org/10.1109/JIOT.2021.3056091

[4] D. E. Lucani, M. StojaNovic, M. Medard, On the Relationship between Transmission Power and Capacity of an Underwater Acoustic Communication Channel, *OCEANS 2008 - MTS/IEEE Kobe Techno-Ocean*, Kobe, Japan, 2008, pp. 1-6. https://doi.org/10.1109/OCEANSKOBE.2008.4531073

[5] H. U. Yildiz, V. C. Gungor, B. Tavli, Packet Size Optimization for Lifetime Maximization in Underwater Acoustic Sensor Networks, *IEEE Transactions on Industrial Informatics*, Vol. 15, No. 2, pp. 719-729, February, 2019. https://doi.org/10.1109/TII.2018.2841830

[6] C.-C. Lin, D.-J. Deng, S.-B. Wang, Extending the Lifetime of Dynamic Underwater Acoustic Sensor Networks Using Multi-Population Harmony Search Algorithm, *IEEE Sensors Journal*, Vol. 16, No. 11, pp. 4034-4042, June, 2016. https://doi.org/10.1109/JSEN.2015.2440416

[7] L. Liu, M. Ma, C. Liu, Y. Shu, Optimal Relay Node Placement and Flow Allocation in Underwater Acoustic Sensor Networks, *IEEE Transactions on Communications*, Vol. 65, No. 5, pp. 2141-2152, May, 2017. https://doi.org/10.1109/TCOMM.2017.2677448

[8] Q. Guan, F. Ji, Y. Liu, H. Yu, W. Chen, Distance-Vector-Based Opportunistic Routing for Underwater Acoustic Sensor Networks, *IEEE Internet of Things Journal*, Vol. 6, No. 2, pp. 3831-3839, April, 2019. https://doi.org/10.1109/JIOT.2019.2891910

[9] C. Zeng, J.-B. Wang, C. Ding, H. Zhang, M. Lin, J. Cheng, Joint Optimization of Trajectory and Communication Resource Allocation for Unmanned Surface Vehicle Enabled Maritime Wireless Networks, *IEEE Transactions on Communications*, Vol. 69, No. 12, pp. 8100-8115, December, 2021. https://doi.org/10.1109/TCOMM.2021.3115115

[10] T. Yang, H. Feng, S. Gao, Z. Jiang, M. Qin, N. Cheng, Two-Stage Offloading Optimization for Energy–Latency Tradeoff With Mobile Edge Computing in Maritime Internet of Things, *IEEE Internet of Things Journal*, Vol. 7, No. 7, pp. 5954-5963, July, 2020. https://doi.org/10.1109/JIOT.2019.2958662

[11] T. Yang, H. Feng, C. Yang, Y. Wang, J. Dong, M. Xia, Multivessel Computation Offloading in Maritime Mobile Edge Computing Network, *IEEE Internet of Things Journal*, Vol. 6, No. 3, pp. 4063-4073, June, 2019. https://doi.org/10.1109/JIOT.2018.2876151

[12] X. Su, H. Y. Xue, Y. Q. Zhou, J. X. Zhu, Research on computing offloading method for maritime observation monitoring sensor network, *Journal on Communications*, Vol. 42, No. 5, pp. 149-163, May, 2021. https://www.joconline.com.cn/thesisDetails#10.11959/j.issn.1000-436x.2021067&lang=en

[13] X. Li, W. Feng, Y. Chen, C.-X. Wang, N. Ge, Maritime Coverage Enhancement Using UAVs Coordinated With Hybrid Satellite-Terrestrial Networks, *IEEE Transactions on Communications*, Vol. 68, No. 4, pp. 2355-2369, April, 2020. https://doi.org/10.1109/TCOMM.2020.2966715

[14] Y. Liu, J. Yan, X. Zhao, Deep Reinforcement Learning Based Latency Minimization for Mobile Edge Computing With Virtualization in Maritime UAV Communication Network, *IEEE Transactions on Vehicular Technology*, Vol. 71, No. 4, pp. 4225-4236, April, 2022. https://doi.org/10.1109/TVT.2022.3141799

[15] R. Ma, R. Wang, G. Liu, W. Meng, X. Liu, UAV-Aided Cooperative Data Collection Scheme for Ocean Monitoring Networks, *IEEE Internet of Things Journal*, Vol. 8, No. 17, pp. 13222-13236, September, 2021. https://doi.org/10.1109/JIOT.2021.3065740

[16] M. Dai, Y. Wu, L. Qian, Z. Su, B. Lin, N. Chen, UAV-Assisted Multi-Access Computation Offloading via Hybrid NOMA and FDMA in Marine Networks, *IEEE Transactions on Network Science and Engineering*, Vol. 10, No. 1, pp. 113-127, January-February, 2023. https://doi.org/10.1109/TNSE.2022.3205303

[17] Z. H. Wei, L. L. Zeng, Edge Computing Offloading Decision Method Based on Stackelberg Game Theory, *Mathematics in Practice and Theory*, Vol. 49, No. 11, pp. 91-100, June, 2019.

Biographies

Yuxuan Ji is currently pursuing the master's degree in telecommunication engineering with the Nanjing University of Posts and Telecommunications, Nanjing, China. Her research interests are in the area of mobile communication

Qi Zhu received the bachelor's and master's degrees in radio engineering from the Nanjing University of Posts and Telecommunications (NUPT), Nanjing, China, in 1986 and 1989, respectively. She is currently a Professor with the School of Telecommunication and Information Engineering, NUPT. Her research interests include wireless networks, Internet of Things, green communication, and mobile edge computing.